Chemical Physics Letters 516 (2011) 162–165

Contents lists available at SciVerse ScienceDirect

Chemical Physics Letters

journal homepage: www.elsevier.com/locate/cplett

A chromophoric study of 2-ethylhexyl *p*-methoxycinnamate

Leonardo F. Alves [a,c], Ricardo Gargano [b], Silvia K.B. Alcanfor [c], Luiz A.S. Romeiro [c,d], João B.L. Martins [a,*]

[a] Instituto de Química, Universidade de Brasília, CP4478, CEP 70919-970 Brasília, DF, Brazil
[b] Instituto de Física, Universidade Brasília, CP04455, CEP 70919-970 Brasília, DF, Brazil
[c] Universidade Católica de Brasília, CEP 71966-700 Brasília, DF, Brazil
[d] Faculdade de Ciências da Saúde, UnB, CEP 70919-970 Brasília, DF, Brazil

ARTICLE INFO

Article history:
Received 31 August 2011
In final form 30 September 2011
Available online 6 October 2011

ABSTRACT

Ultraviolet absorption spectra of 2-ethylhexyl *p*-methoxycinnamate have been recorded in different solvents and calculated using the time dependent density functional theory. The calculations were performed with the aid of B3LYP, PBE1PBE, M06, and PBEPBE functionals and 6-31+G(2d) basis set. The geometries were initially optimized using PM5 semiempirical method for the conformational search. The calculations of excited states were carried out using the time dependent with IEF-PCM solvent reaction field method. The experimental data were obtained in the wavelength range from 200 to 400 nm using 10 different solvents. The TD-PBE1PBE method shows the best agreement to the experimental results.

1. Introduction

Ultraviolet (UV) radiation reaching the earth surface can be divided into three regions: (i) UVA (320–400 nm) which comprises 95–99% [1] of the UV radiation that reach the surface and a small amount of UVB (290–320 nm), while UVC (200–290 nm) is filtered out by the atmosphere. The UV radiation present in sunlight is the primary cause of non-melanoma skin cancer [2]. Although the role of UVB in inducing skin cancer and immune suppression is well known [2], the contribution of UVA to the deleterious effects of sunlight are related to dermatoheliosis (photoaging), where it penetrates deeper into the skin (160–250 μm) than UVB radiation (17–49 μm) reaching the vascular network.

Therefore, in recent years, skin cancers, particularly melanomas, have become an important public health issue and there has been a considerable interest of new sunscreen products. The required feature of sunscreens is to spread and block the solar UV light from UVB/UVA range (290–400 nm) avoiding it to penetrate in the skin.

In order to minimize the effects of ultraviolet radiations to the skin, some compounds with particular chromophores have been used in the photoprotectors. Formulations of sunscreens can be divided into organic absorbers and inorganic blockers on the basis of their mechanism of action [1]. The organic compounds absorb UV rays with excitation to a higher energy state, which can be represented by *p*-aminobenzoic acid, salicylates, cinnamates, benzophenones, butylmethoxydibenzoylmethane, drometrizole, and trisulfonic acid. The inorganic agents include titanium dioxide and zinc oxide, which can offer some visible light protection by reflecting and/or scattering most of the UV-rays through its high refractive index [3].

2-Ethylhexyl (2E)-3-(4-methoxyphenyl)prop-2-enoate – also known as 2-ethylhexyl *p*-methoxycinnamate and octyl *p*-methoxycinnamate (OMC) is the most common cinnamate and probably the most common UV filter used globally (λ_{max}, 311 nm) [4]. The behavior of OMC in light has been the subject of several papers [1,4].

The aim of this Letter is to study the ultraviolet spectrum of OMC molecule, using the TD-DFT method based on generalized gradient approximation (GGA) functionals, and analyzes the solvent effects of the experimental data collected in the wavelength range from 200 to 400 nm. This theoretical study is inserted in the scope of a research program aiming to design, synthesize, and perform effectiveness evaluation of new UV absorbing agents. In this case, it will contribute to the optimization of the new compounds.

2. Computational details

Theoretical prediction of absorption spectra for polyatomic systems requires some compromise between computational cost and accuracy. Time dependent (TD) is the least expensive method for systems of large number of atoms without including multielectron excitations. TD density functional theory (DFT) using hybrid DFT/HF approach, based on the Becke's three-parameter hybrid method by means of the Lee–Yang–Parr correlation functional (B3LYP), and the Perdew–Burke–Erzenrhof exchange–correlation functional (PBE1PBE), were recently applied to calculate geometrical optimizations and vertical transitions from ground to the low-lying

* Corresponding author. Address: Universidade de Brasília, CP 4478, CEP 70904-970 Brasília, DF, Brazil. Fax: +55 61 31073900.
E-mail address: lopes@unb.br (J.B.L. Martins).

0009-2614
doi:10.1016/j.cplett.2011.09.078

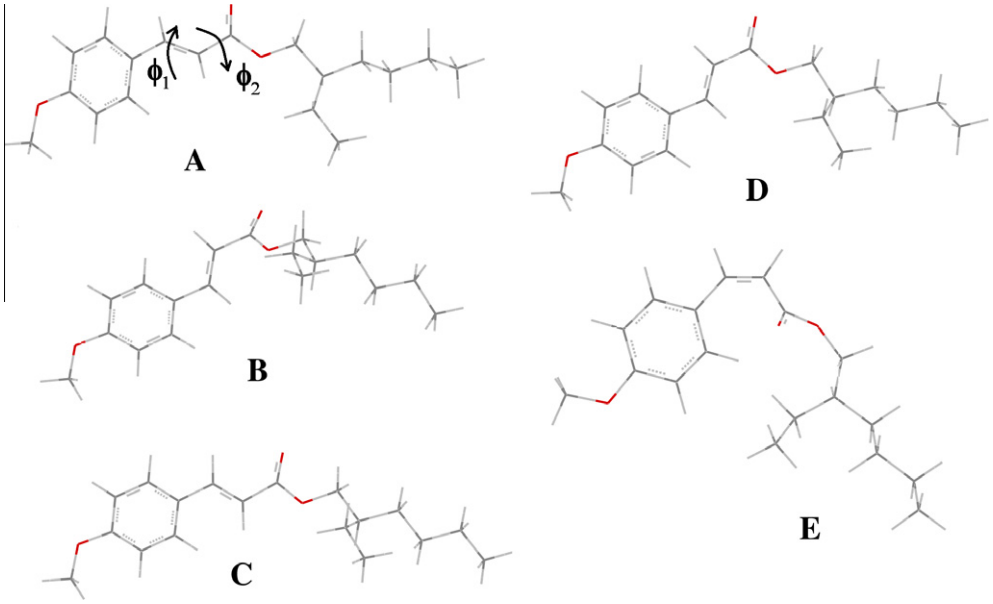

Figure 1. Conformational study of OMC molecules. The dihedral angles (ϕ1, ϕ2) were used for the conformational search.

Table 1
Absorption wavelength and energy difference of four lowest stable configurations of OMC at TD-PBE1PBE/6-31+G(2d)//PM5 level. The dihedral angles (degrees) and A, B, C, D, E structures were shown in Figure 1.

		A	B	C	D	E
ϕ_1 (°)		−179.8	179.1	−178.9	178.5	−1.4
ϕ_2 (°)		165.0	165.0	−45.0	15.0	113.9
Wavelength absorption (nm)	Acetone	301	308	293	304	281
	Benzene	298	306	292	301	281
	DMSO	302	310	294	306	282
	Ethanol	301	308	293	304	281
Energy difference* (kJ/mol)	Acetone	6.42	0.00	13.29	4.76	70.29
	Benzene	5.92	0.00	13.95	3.96	61.87
	DMSO	6.52	0.00	13.21	4.87	70.95
	Ethanol	6.58	0.00	13.32	4.90	70.79

* The (total) energy difference is in relation to the most stable B isomer.

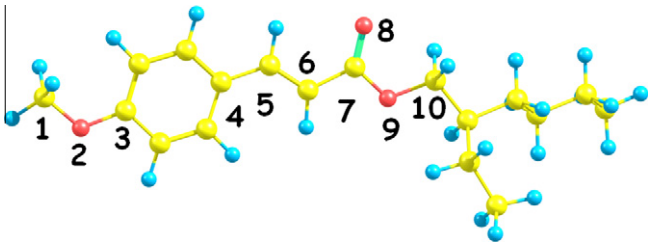

Figure 2. Optimized geometry at PBE1PBE/6-31+G(2d) level.

singlet electronic excited states with agreement to the experimental data [5,6]. The hybrid meta exchange correlation functional, called M06 [7] and the pure PBEPBE functional were also used.

The conformational search was carried out with PM5 semiempirical method, available in the CACHE program [8]. The minimum energy conformation was used for the optimization at PBE1PBE/6-31+G(2d), B3LYP/6-31+G(2d), PBEPBE/6-31+G(2d), and M06/6-31+G(2d) levels of theory. These optimized geometries were used for the TD-DFT calculation of the excited states. TD-DFT calculations have shown a good comparison to experimental absorption

Table 2
Interatomic distances (Å), bond (α), and dihedral angles (ϕ) (degrees) of OMC. See Figure 2 for the labels.

OMC	PBE1PBE/6-31+G(2d)	B3LYP/6-31+G(2d)	PBEPBE/6-31+G(2d)	M06/6-31+G(2d)	Experimental*
d(C1–O2)	1.4092	1.4202	1.4282	1.4074	1.417
d(O2–C3)	1.3498	1.3584	1.3642	1.3500	1.357
d(C7=O8)	1.2100	1.2143	1.2249	1.2086	1.194
d(C7–O9)	1.3460	1.3552	1.3702	1.3472	1.324
d(O9–C10)	1.4286	1.4413	1.4471	1.4278	1.452
α(1-2-3)	118.08	118.62	117.75	118.20	118.12
α(7-9-10)	115.81	116.38	115.32	116.00	116.19
ϕ(4–5–6–7)	179.55	179.95	179.94	179.91	176.61
ϕ(5–6–7–9)	179.55	179.92	179.99	179.77	174.06

* Experimental data from the MMC molecule [14].

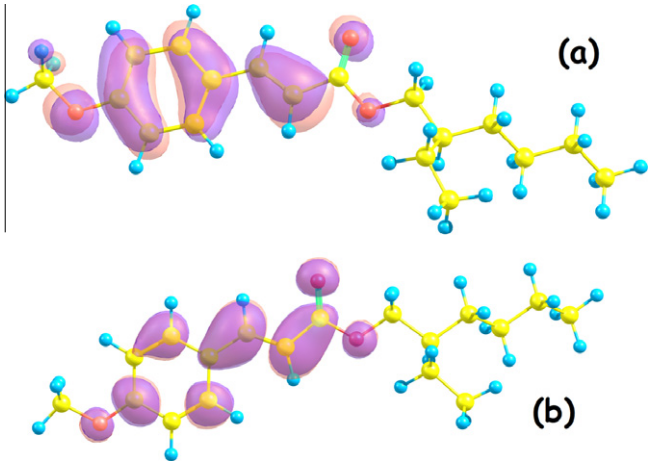

Figure 3. (a) HOMO orbital and (b) LUMO orbital of OMC molecule optimized at PBE1PBE/6-31+G(2d) level.

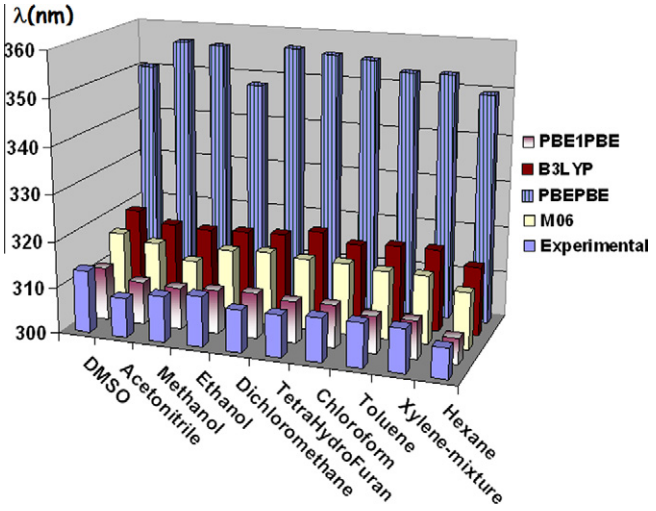

Figure 4. Theoretical results of solvent effects on absorption wavelengths compared to the experimental data.

wavelengths [9]. Initially, they have been calculated in the vacuum, then the solvent effects on the excitation energies were computed through the integral equation formalism of the polarizable continuum model (IEF-PCM) [10], into the consistent reaction field, where the solvent is taken into account by means of a polarizable dielectric medium. The solvents used are the following: dimethyl sulfoxide (DMSO), acetonitrile, methanol, ethanol, acetone, dichloroethane, dichloromethane, tetrahydrofuran, chloroform, *o*-xylene, toluene, xylene-mixture, *m*-xylene, *p*-xylene, benzene, and hexane. The TD and DFT calculations were performed using the GAUSSIAN 09 program package [11].

3. Experimental details

The stock solutions were prepared starting with 0,2 mg of 2-ethylhexyl-4-methoxycinnamate, measured on an analytical balance (semi-micro), diluted in 10 mL of the following solvents acetonitrile (ACS, 99.9%), absolute ethanol (ACS/USP, 99.9%), methanol (HPLC/SPECTRO, 99.99%), chloroform (ACS, 99.8%), dichloromethane (ACS, 99.5%), hexane (ACS, 95.0%), tetrahydrofuran (HPLC/SPECTRO, 99.8%), and xylene (ACS, 98.5%) purchased from TEDIA; toluene (ACS/ISO; 99.5%) from Merck and dimethylsulfoxide (ACS, 99.9%) from Synth. These stock solutions were further diluted in their respective solvents using 125 μL of each solution to 5 mL to give final concentration of 0,5 mg L^{-1}. The spectra were obtained on Cary 50 Varian spectrophotometer in the wavelength range from 200 to 400 nm with a scan rate of 60 nm/min and error of ±0.5 nm.

4. Results and discussions

Firstly, we have carried out a conformational study of OMC using the PM5 semiempirical method. Two dihedral angles were scanned in order to find the lowest stable conformations. The PM5 optimized molecules of five lowest energies (Figure 1) from the conformational search were taken for the calculation of absorption wavelength at TD-PBE1PBE/6-31+G(2D) level with four different solvents, acetone, benzene, DMSO, and ethanol (Table 1). A and B are *trans* isomers (in regard to the C=C bond), while C, D, and E are *cis* isomers. Table 1 also shows the energy difference of A, C, D, and E isomers in relation to the B isomer. The B isomer, almost planar *trans–trans* structure, showed the lowest energy and was used for the optimization using different functionals. The wavelength absorption for the B *trans* isomer is in accordance to the experimental value of 310 nm in ethanol while the *cis* isomer has an experimental absorption value of 301 nm [4,12]. Therefore, the

Table 3
Absorption wavelengths (nm) and oscillator strength (in parenthesis) of OMC molecule at TD-DFT/6-31+G(2d)//DFT/6-31+G(2d) level.

	PBE1PBE	B3LYP	PBEPBE	M06	Experimental
DMSO	310 (1.021)	321 (0.993)	358 (0.898)	317 (0.967)	313
Acetonitrile	309 (1.008)	319 (0.982)	356 (0.884)	315 (0.954)	308
Methanol	309 (1.005)	319 (0.977)	356 (0.881)	315 (0.951)	310
Ethanol	309 (1.011)	319 (0.983)	356 (0.888)	316 (0.957)	311
Acetone	309 (1.010)	319 (0.982)	356 (0.888)	315 (0.957)	–
Dichloroethane	310 (1.024)	320 (0.997)	357 (0.905)	316 (0.969)	–
Dichloromethane	309 (1.021)	320 (0.993)	356 (0.902)	316 (0.966)	309
Tetrahydrofuran	309 (1.017)	319 (0.990)	356 (0.899)	315 (0.962)	309
Chloroform	309 (1.022)	319 (0.996)	355 (0.908)	315 (0.967)	309
o-Xylene	308 (1.029)	318 (1.003)	353 (0.914)	315 (0.971)	–
Toluene	308 (1.027)	318 (1.001)	353 (0.920)	315 (0.969)	309
Xylene-mixture	308 (1.028)	318 (1.002)	353 (0.920)	315 (0.970)	309
m-Xylene	308 (1.027)	318 (1.002)	353 (0.920)	315 (0.969)	–
p-Xylene	308 (1.027)	318 (1.001)	353 (0.920)	315 (0.969)	–
Benzene	308 (1.028)	318 (1.002)	353 (0.921)	315 (0.969)	–
Hexane	305 (1.006)	315 (0.980)	349 (0.899)	312 (0.947)	306
Vacuum	295 (0.896)	302 (0.871)	336 (0.788)	302 (0.836)	–

This table is written in order of decreasing solvent dielectric constant.

absorption maxima depend on the polarity of the used solvent. The equilibrium shifted to higher concentration *trans* OMC when less polar solvent was used, as *trans* OMC is more hydrophobic than *cis* OMC [12]. It is expected that λ_{max} *cis*-isomer is less than λ_{max} *trans*-isomer [13], which was shown by the calculated values for the *cis* and *trans* isomers (Table 1).

The singlet electronic ground state geometry of OMC molecule (Figure 2) was firstly optimized in vacuum using DFT. In general, the optimized geometries show similar results among the methods used, then only the PBE1PBE results were depicted in Figure 2. Table 2 shows the optimized geometry results for the B isomer at different levels of theory. The interatomic distance has a highest mean standard deviation of 0.0172 Å, while the highest standard mean deviation of angles is 1.13°. Presently, there is no available experimental data of OMC structure, then the data of methyl 3-(4-methoxyphenyl) prop-2-enoate or methyl *p*-methoxycinnamate (MMC) [14] which have similar chromophore structure (carbon C1 through C13) centers was used to analyze the theoretical results. The MMC has slightly smaller values of interatomic distances than the results obtained with DFT methods; the exception is the carbon ester terminal, OCH_3. The largest absolute deviation was found for the second dihedral angle, of almost 6°. Therefore, the obtained geometries are in agreement with the experimental result of MMC. The ground state DFT wave function of OMC consists of 79 occupied orbitals. The HOMO (highest occupied molecular orbital) is mainly π orbital and the LUMO is mainly π^* antiligant orbital (Figure 3). These results suggest that there is no charge transfer for the HOMO–LUMO transition. Lone pairs are also shown in Figure 3.

We have calculated the vertical transition, i.e., the Franck–Condon principle, where the electronic transition is carried out without changes in the nuclear positions. Table 3 shows the TD vertical electronic transition wavelengths for the optimized geometries using the 6-31+G(2D) basis set, the IEF-PCM solvent model, and the B3LYP, PBE1PBE, PBEPBE, and M06 DFT functionals. The experimental absorption data are also shown in Table 3 for the following solvents: acetonitrile, methanol, ethanol, dichloromethane, tetrahydrofuran, chloroform, toluene, xylene, and hexane. Often, the maximum absorption wavelength of OMC was usually subjected to solvent effects, in which bathochromic shifts were observed in more polar solvents [12]. A small red shift of the wide band is observed when the solvent polarity is increased, indicating that this band is the result of a π–π^* transition. Otherwise, peaks resulting from $n \rightarrow \pi^*$ transitions are shifted to shorter wavelengths as the solvent polarity increase, due to the solvation of lone pairs. Therefore, the results mainly suggest $\pi \rightarrow \pi^*$ contribution for this transition, and the charge transfer remains on the same chromophoric site. The pure density functional, PBEPBE, shows the largest wavelength absorption for all studied solvents, while PBE1PBE gives the smallest values, and M06 has the same trend of B3LYP. Therefore, the hybrid functionals show better agreement compared to the experimental absorption wavelength than the pure functional. These results are in accordance to the theoretical studies that report pure functionals with largest wavelength absorption [15]. Our experimental data show agreement with the literature for acetonitrile (308 nm [16]), methanol (310 nm [16] and 309 nm [17]), ethanol (310 nm [12]), dichloromethane (310 nm [16]), tetrahydrofuran (308 nm [16]), and toluene (309 nm [17]). There is also an agreement of the calculated data with our experimental results (Figure 4). In general, the experimental spectra show a mean value for the maximum absorption at almost 310 nm in accordance to the mean value of 309 nm for the literature [12,16,17], excepting the hexane solvent which has a different behavior with maximum absorption in 290 nm [12], which is in contrast to our experimental result of 306 nm. Otherwise this experimental value is in better accordance to the PBE1PBE value of 305 nm than the one from the literature. Despite the solvation model is implicit, i.e., the solvent is taken into account by means of a polarizable dielectric medium, IEF-PCM reproduces the qualitative effects of solvatochromic shifts.

5. Conclusions

We have carried out TD-DFT with IEF-PCM solvent model and recorded the ultraviolet absorption spectra of 2-ethylhexyl-4-methoxycinnamate. Several functionals were employed: PBE1PBE, B3LYP, PBEPBE, and M06 methods with 6-31+G(2d) basis set.

The TD-PBE1PBE method shows the best agreement to the experimental results and the main energy absorption is due to the HOMO–LUMO transition. The results mainly suggest $\pi \rightarrow \pi^*$ contribution for this transition. M06 and B3LYP show basically the same behavior, while pure functionals have the largest absorption wavelength.

Acknowledgments

The authors are indebted to the financial support of CNPq, INCTMN, and CAPES.

References

[1] C. Antoniou, M.G. Kosmadaki, A.J. Stratigos, A.D. Katsambas, J. Eur. Acad. Dermatol. Venereol. 22 (2008) 1110.
[2] D.X. Nghiem, N. Kazimi, G. Clydesdale, H.N. Ananthaswamy, M.L. Kripke, S.E. Ullrich, J. Invest. Dermatol. 117 (2001) 1193.
[3] H. Yang, S. Zhu, N. Pan, J. Appl. Polym. Sci. 92 (2004) 3201.
[4] S.P. Huong, V. Andrieu, J.P. Reynier, E. Rocher, J.D. Fourneron, J. Photochem. Photobiol. A 186 (2007) 65.
[5] C. Zazza, A. Grandi, L. Bencivenni, M. Aschi, Theochem. J. Mol. Struct. 764 (2006) 87.
[6] N.L. Marana, V.M. Longo, E. Longo, J.B.L. Martins, J.R. Sambrano, J. Phys. Chem. A 112 (2008) 8958.
[7] Y. Zhao, D.G. Truhlar, Theor. Chem. Account. 120 (2008) 215.
[8] Cache, Cache Workspace 7.5. Fujtisu, 2002.
[9] J.B.L. Martins, J.A. Duraes, M.J.A. Sales, A.F.A. Vilela, G.M.E. Silva, R. Gargano, Int. J. Quantum Chem. 109 (2009) 739.
[10] J. Tomasi, B. Mennucci, R. Cammi, Chem. Rev. 105 (2005) 2999.
[11] M.J. Frisch et al., Gaussian 09, Revision A.02, Gaussian, Inc., Wallingford CT, 2009.
[12] S. Pattanaargson, T. Munhapol, N. Hirunsupachot, P. Luangthongaram, J. Photochem. Photobiol. A 161 (2004) 269.
[13] G.J. Smith, I.J. Miller, J. Photochem. Photobiol. A 118 (1998) 93.
[14] P. Luger, M. Weber, N.X. Dung, N.T.B. Tuyet, Acta Crystallogr. C 52 (1996) 1255.
[15] Y. Shigemitsua, K. Komiya, N. Mizuyama, Y. Tominaga, Theochem. J. Mol. Struct. 855 (2008) 92.
[16] L. Beyere, S. Yarasi, G.R. Loppnow, J. Raman Spectrosc. 34 (2003) 743.
[17] R. Krishnan, A. Carr, E. Blair, T.M. Nordlund, Photochem. Photobiol. 79 (2004) 531.